Lattice QCD Study for the Interquark Force in Three-Quark and Multi-Quark Systems

H. Suganuma*, T.T. Takahashi†, F. Okiharu** and H. Ichie*

*Faculty of Science, Tokyo Institute of Technology, Tokyo 152-8551, Japan
†Yukawa Institute for Theoretical Physics, Kyoto University, Kyoto 606-8502, Japan
**Department of Physics, Nihon University, Kanda-Surugadai 1-8, Chiyoda, Tokyo 101, Japan

Abstract. We study three-quark and multi-quark potentials in SU(3) lattice QCD. From accurate calculations for more than 300 different patterns of 3Q systems, the static ground-state 3Q potential $V_{3Q}^{g.s.}$ is found to be well described by the Coulomb plus Y-type linear potential (Y-Ansatz) within 1%-level deviation. As a clear evidence for Y-Ansatz, Y-type flux-tube formation is actually observed on lattices in maximally-Abelian projected QCD. For about 100 patterns of 3Q systems, we perform accurate calculations for the 1st excited-state 3Q potential $V_{3Q}^{e.s.}$ by diagonalizing the QCD Hamiltonian in presence of three quarks, and find a large gluonic-excitation energy $\Delta E_{3Q} \equiv V_{3Q}^{e.s.} - V_{3Q}^{g.s.}$ of about 1 GeV, which gives a physical reason on success of the quark model. ΔE_{3Q} is found to be reproduced by "inverse Mercedes Ansatz", which indicates a complicated bulk excitation for the gluonic-excitation mode. We study also tetra-quark and penta-quark potentials in lattice QCD, and find that they are well described by the OGE Coulomb plus multi-Y type linear potential, which supports the flux-tube picture even for multi-quarks. Finally, narrow decay width of low-lying penta-quark baryons is discussed in terms of the QCD string theory.

Keywords: lattice QCD, inter-quark potential, multi-quark, gluonic excitation, confinement, string
PACS: 12.38.Gc, 12.38.Aw, 12.39.Mk, 12.39.Jh, 12.39.Pn, 13.30.Eg, 14.20.Jn, 11.25.Wx

1. INTRODUCTION

Quantum chromodynamics (QCD), an SU(3) gauge theory, was first proposed by Yoichiro Nambu [1] in 1966 as a candidate for the fundamental theory of strong interaction, just after introduction of a "new" quantum number, "color" [2]. In spite of its simple form, QCD creates thousands of hadrons and leads to various interesting nonperturbative phenomena such as color confinement [3, 4, 5] and dynamical chiral-symmetry breaking [6]. Even at present, it is very difficult to deal with QCD analytically due to its strong-coupling nature in an infrared region. Instead, lattice QCD has been applied as a direct numerical analysis for nonperturbative QCD.

In 1979, the first application [7] of lattice QCD Monte Carlo simulations was done for the inter-quark potential between a quark and an antiquark using the Wilson loop. Since then, the study of inter-quark forces has been one of the important issues in lattice QCD [8]. Actually, in hadron physics, the inter-quark force can be regarded as an elementary quantity to connect the "quark world" to the "hadron world", and plays an important role to hadron properties.

In this paper, we perform detailed and high-precision analyses for inter-quark forces in three-quark and multi-quark systems with SU(3) lattice QCD [9, 10, 11, 12, 13, 14, 15, 16, 17], and try to extract the proper picture for hadrons including multi-quarks.

CP756, *Quark Confinement and the Hadron Spectrum VI*
edited by N. Brambilla, U. D'Alesio, A. Devoto, K. Maung, G.M. Prosperi and S. Serci

2. THE THREE-QUARK POTENTIAL IN LATTICE QCD

In general, three-body forces are regarded as residual interaction in most fields in physics. In QCD, however, the three-body force among three quarks is a "primary" force reflecting SU(3) gauge symmetry. In fact, the three-quark (3Q) potential is directly responsible for structure and properties of baryons, similar to the relevant role of the $Q\bar{Q}$ potential for meson properties. Furthermore, the 3Q potential is a key quantity to clarify quark confinement in baryons. However, in contrast to the $Q\bar{Q}$ potential [8], there were only a few pioneering lattice studies [18] done in 80's for the 3Q potential before our study in 1999 [9], in spite of its importance in hadron physics.

As for the functional form of the inter-quark potential, we note two theoretical arguments at short and long distance limits.

1. At short distances, perturbative QCD is applicable, and therefore the inter-quark potential is expressed as the sum of two-body OGE Coulomb potentials.
2. At long distances, the strong-coupling expansion of QCD is plausible, and it leads to the flux-tube picture [19].

Then, we theoretically conjecture the functional form of the inter-quark potential as the sum of OGE Coulomb potentials and a linear potential based on the flux-tube picture,

$$V = \frac{g^2}{4\pi} \sum_{i<j} \frac{T_i^a T_j^a}{|\mathbf{r}_i - \mathbf{r}_j|} + \sigma L_{\min} + C, \tag{1}$$

where $L_{\min}$ is the minimal value of the total length of flux-tubes linking static quarks. Of course, it is highly nontrivial that these simple arguments on UV and IR limits of QCD hold for intermediate distances. Nevertheless, lattice QCD indicates that the $Q\bar{Q}$ potential $V_{Q\bar{Q}}(r)$ is well described with this form as [8, 10, 11]

$$V_{Q\bar{Q}}(r) = -\frac{A_{Q\bar{Q}}}{r} + \sigma_{Q\bar{Q}} r + C_{Q\bar{Q}}. \tag{2}$$

For 3Q systems, there appears a junction which connects three flux-tubes from three quarks, and Y-type flux-tube formation is expected [10, 11, 19, 20, 21]. Therefore, the (ground-state) 3Q potential is expected to be the Coulomb plus Y-type linear potential, i.e., Y-Ansatz,

$$V_{3Q}^{\text{g.s.}} = -A_{3Q} \sum_{i<j} \frac{1}{|\mathbf{r}_i - \mathbf{r}_j|} + \sigma_{3Q} L_{\min} + C_{3Q}, \tag{3}$$

where $L_{\min}$ is Y-shaped flux-tube length.

For more than 300 different patterns of spatially-fixed 3Q systems, we calculate the ground-state 3Q potential $V_{3Q}^{\text{g.s.}}$ from the 3Q Wilson loop W_{3Q} using SU(3) lattice QCD [10, 11, 12, 13] with the standard plaquette action at the quenched level on various lattices, i.e., (β=5.7, $12^3 \times 24$), (β=5.8, $16^3 \times 32$), (β=6.0, $16^3 \times 32$) and ($\beta = 6.2, 24^4$). For accurate measurements, we construct ground-state-dominant 3Q operators using the smearing method [10, 11]. Note that the lattice QCD calculation is completely independent of any Ansatz for the potential form.

To conclude, we find that the static ground-state 3Q potential $V_{3Q}^{g.s.}$ is well described by the Coulomb plus Y-type linear potential (Y-Ansatz) within 1%-level deviation [10, 11]. To demonstrate this, we show in Fig.1(a) 3Q confinement potential V_{3Q}^{conf}, i.e., the 3Q potential subtracted by its Coulomb part, plotted against Y-shaped flux-tube length L_{min}. For each β, clear linear correspondence is found between 3Q confinement potential V_{3Q}^{conf} and L_{min}, which indicates Y-Ansatz for the 3Q potential.

Recently, as a clear evidence for Y-Ansatz, Y-type flux-tube formation is actually observed in maximally-Abelian (MA) projected lattice QCD from measurements of the action density in spatially-fixed 3Q systems [14, 22]. (See Figs.1 (b) and (c).) In this way, together with recent several analytical studies [23, 24], Y-Ansatz for the static 3Q potential seems to be almost settled.

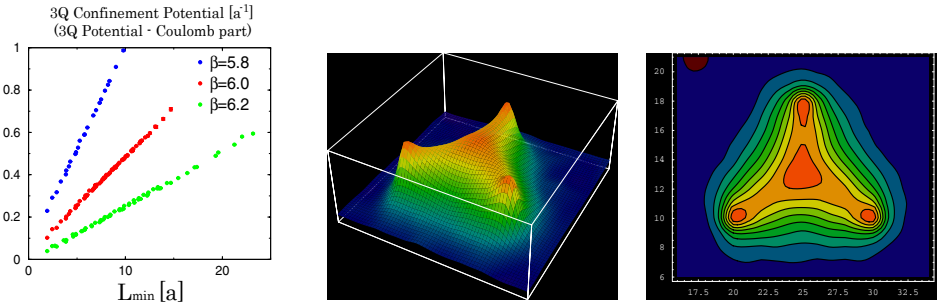

FIGURE 1. (a) 3Q confinement potential V_{3Q}^{conf}, i.e., the 3Q potential subtracted by its Coulomb part, plotted against Y-shaped flux-tube length L_{min} at β=5.8, 6.0 and 6.2 in the lattice unit. (b) A bird's-eye view and (c) a contour map of the lattice QCD result for Y-type flux-tube formation in a spatially-fixed 3Q system in MA projected QCD. The distance between the junction and each quark is about 0.5 fm.

3. GLUONIC EXCITATIONS IN 3Q SYSTEMS

In this section, we study excited-state 3Q potentials and gluonic excitations in 3Q systems using lattice QCD [12, 13]. The excited-state 3Q potential $V_{3Q}^{e.s.}$ is the energy of the excited state in the static 3Q system. The energy difference $\Delta E_{3Q} \equiv V_{3Q}^{e.s.} - V_{3Q}^{g.s.}$ between $V_{3Q}^{g.s.}$ and $V_{3Q}^{e.s.}$ is called as the gluonic-excitation energy, and physically means the excitation energy of the gluon-field configuration in the static 3Q system. In hadron physics, the gluonic excitation is one of interesting phenomena beyond the quark model, and relates to hybrid hadrons such as $q\bar{q}G$ and $qqqG$ in the valence picture.

For about 100 different patterns of 3Q systems, we calculate the excited-state potential in SU(3) lattice QCD with $16^3 \times 32$ at β=5.8 and 6.0 at the quenched level by diagonalizing the QCD Hamiltonian in presence of three quarks. In Fig.2, we show the 1st excited-state 3Q potential $V_{3Q}^{e.s.}$ and the ground-state potential $V_{3Q}^{g.s.}$. The gluonic excitation energy $\Delta E_{3Q} \equiv V_{3Q}^{e.s.} - V_{3Q}^{g.s.}$ in 3Q systems is found to be about 1GeV in hadronic scale as $0.5\text{fm} \leq L_{min} \leq 1.5\text{fm}$. Note that the gluonic excitation energy of about 1GeV is rather large compared with excitation energies of quark origin. This result predicts that the lowest hybrid baryon $qqqG$ has a large mass of about 2 GeV.

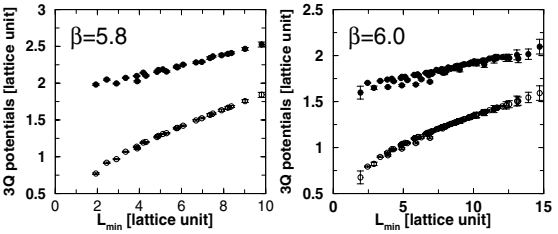

FIGURE 2. The 1st excited-state 3Q potential $V_{3Q}^{\text{e.s.}}$ and the ground-state 3Q potential $V_{3Q}^{\text{g.s.}}$. The lattice results at $\beta = 5.8$ and $\beta = 6.0$ well coincide apart from an irrelevant overall constant. The gluonic excitation energy $\Delta E_{3Q} \equiv V_{3Q}^{\text{e.s.}} - V_{3Q}^{\text{g.s.}}$ is about 1GeV in hadronic scale as $0.5\text{fm} \leq L_{\min} \leq 1.5\text{fm}$.

Inverse Mercedes Ansatz for Gluonic Excitations in 3Q Systems

Next, we investigate the functional form of $\Delta E_{3Q} \equiv V_{3Q}^{\text{e.s.}} - V_{3Q}^{\text{g.s.}}$, where the Coulomb part is expected to be canceled between $V_{3Q}^{\text{g.s.}}$ and $V_{3Q}^{\text{e.s.}}$. After some trials, as shown in Fig.3, we find that the lattice data of the gluonic excitation energy $\Delta E_{3Q} \equiv V_{3Q}^{\text{e.s.}} - V_{3Q}^{\text{g.s.}}$ are relatively well reproduced by "inverse Mercedes Ansatz" [13],

$$\Delta E_{3Q} = \frac{K}{L_{\bar{\Upsilon}}} + G, \quad L_{\bar{\Upsilon}} \equiv \sum_{i=1}^{3} \sqrt{x_i^2 - \xi x_i + \xi^2} = \frac{1}{2} \sum_{i \neq j} \overline{\mathrm{P_i Q_j}} \quad (x_i \equiv \overline{\mathrm{PQ}}_i,\ \xi \equiv \overline{\mathrm{PP}}_i), \quad (4)$$

where $L_{\bar{\Upsilon}}$ denotes "modified Y-length" defined by a half perimeter of "Mercedes form" as shown in Fig.3(a). As for (K, G, ξ), we find ($K \simeq 1.43$, $G \simeq 0.77$ GeV, $\xi \simeq 0.116$ fm) at $\beta = 5.8$, and ($K \simeq 1.35$, $G \simeq 0.85$ GeV, $\xi \simeq 0.103$ fm) at $\beta = 6.0$.

Inverse Mercedes Ansatz indicates that the gluonic-excitation mode is realized as a complicated bulk excitation of the whole 3Q system.

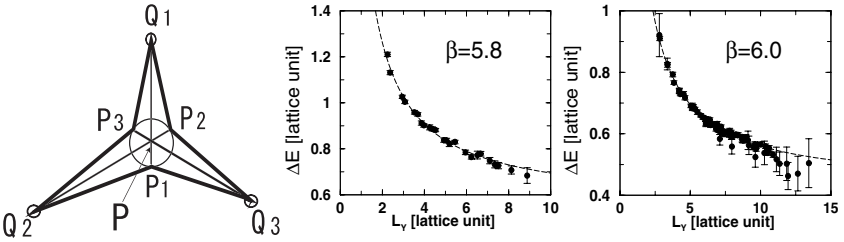

FIGURE 3. (a) Mercedes form for a 3Q system. (b) Lattice QCD results of the gluonic excitation energy $\Delta E_{3Q} \equiv V_{3Q}^{\text{e.s.}} - V_{3Q}^{\text{g.s.}}$ in 3Q systems plotted against modified Y-length $L_{\bar{\Upsilon}}$ at $\beta = 5.8$. (c) The same at β=6.0. The dashed curve denotes inverse Mercedes Ansatz.

Behind Success of the Quark Model

Here, we consider connection between QCD and the quark model in terms of gluonic excitations [12, 13, 14, 15]. While QCD is described with quarks and gluons, the simple

quark model successfully describes low-lying hadrons even without explicit gluonic modes. In fact, gluonic excitations seem invisible in low-lying hadron spectra, which is rather mysterious.

On this point, we find the gluonic-excitation energy to be about 1GeV or more, which is rather large compared with excitation energies of quark origin. Therefore, contribution of gluonic excitations is considered to be negligible and dominant contribution is brought by quark dynamics such as spin-orbit interaction for low-lying hadrons. Thus, the large gluonic-excitation energy of about 1GeV gives a physical reason for the invisible gluonic excitation in low-lying hadrons, which would play a key role for success of the quark model without gluonic modes [12, 13, 14, 15].

In Fig.4, we present a possible scenario from QCD to the massive quark model in terms of color confinement and dynamical chiral-symmetry breaking (DCSB).

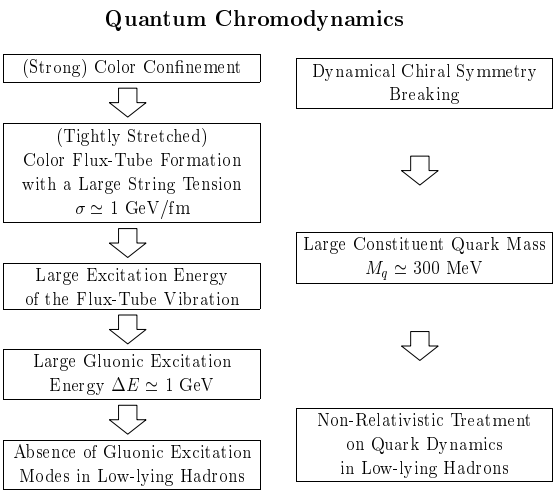

FIGURE 4. A possible scenario from QCD to the quark model in terms of color confinement and DCSB. DCSB leads to a large constituent quark mass of about 300 MeV, which enables non-relativistic treatment for quark dynamics approximately. Color confinement results in color flux-tube formation among quarks with a large string tension of $\sigma \simeq 1$ GeV/fm. In the flux-tube picture, gluonic excitations are described as flux-tube vibrations, which are expected to be large in hadronic scale. Indeed, the large gluonic-excitation energy of about 1 GeV observed in lattice QCD leads to absence of gluonic modes in low-lying hadrons, which plays a key role to success of the quark model without gluonic excitation modes.

4. TETRA-QUARK AND PENTA-QUARK POTENTIALS

In this section, we perform the first study of multi-quark potentials in SU(3) lattice QCD, motivated by recent experimental discoveries of multi-quark hadrons, i.e., X(3872) and $D_s(2317)$ as candidates of tetra-quark (QQ-$\bar{\mathrm{Q}}\bar{\mathrm{Q}}$) mesons, and $\Theta^+(1540)$, $\Xi^{--}(1862)$ and $\Theta_c(3099)$ as penta-quark (4Q-$\bar{\mathrm{Q}}$) baryons [25]. As unusual features of multi-quark hadrons, their decay widths are extremely narrow, e.g., $\Gamma(\mathrm{X}(3872)) < 2.3$MeV (90% C.L.). For physical understanding of multi-quark hadrons, theoretical analyses are nec-

essary as well as experimental studies. In particular, for realistic model calculations of multi-quark hadrons, it is required to clarify inter-quark forces such as the quark confinement force in multi-quark systems based on QCD.

OGE Coulomb plus Multi-Y Ansatz

As a theoretical form of the multi-quark potential, we present one-gluon-exchange (OGE) Coulomb plus multi-Y Ansatz [15, 16, 17] based on Eq.(1), i.e., the sum of OGE Coulomb potentials and the linear confinement potential proportional to multi-Y-shaped flux-tube length $L_{\rm min}$.

On the 4Q potential $V_{\rm 4Q}$, we investigate QQ-$\bar{\rm Q}\bar{\rm Q}$ systems where two quarks locate at ($\mathbf{r}_1$, $\mathbf{r}_2$) and two antiquarks at ($\mathbf{r}_3$, $\mathbf{r}_4$) as shown in Fig.5. For connected 4Q systems, a plausible form of $V_{\rm 4Q}$ is OGE plus multi-Y Ansatz [17],

$$V_{\rm c4Q} \equiv -A_{\rm 4Q}\{(\frac{1}{r_{12}}+\frac{1}{r_{34}})+\frac{1}{2}(\frac{1}{r_{13}}+\frac{1}{r_{14}}+\frac{1}{r_{23}}+\frac{1}{r_{24}})\}+\sigma_{\rm 4Q}L_{\rm min}+C_{\rm 4Q}, \qquad (5)$$

while $V_{\rm 4Q}$ for disconnected 4Q systems would be approximated by "two-meson" Ansatz as $V_{\rm 2Q\bar{Q}} \equiv V_{\rm Q\bar{Q}}(r_{13})+V_{\rm Q\bar{Q}}(r_{24})$.

On the 5Q potential $V_{\rm 5Q}$, we investigate QQ-$\bar{\rm Q}$-QQ systems where the two quarks at ($\mathbf{r}_1$, $\mathbf{r}_2$) and those at ($\mathbf{r}_3$, $\mathbf{r}_4$) form $\bar{\mathbf{3}}$ representation of SU(3) color, respectively, and the antiquark locates at $\mathbf{r}_5$, as shown in Fig.5. For the 5Q system, OGE Coulomb plus multi-Y Ansatz is expressed as $V_{\rm 5Q} = V_{\rm 5Q}^{\rm Coul}+\sigma_{\rm 5Q}L_{\rm min}+C_{\rm 5Q}$ with the Coulomb part as

$$V_{\rm 5Q}^{\rm Coul} = -A_{\rm 5Q}\{(\frac{1}{r_{12}}+\frac{1}{r_{34}})+\frac{1}{2}(\frac{1}{r_{15}}+\frac{1}{r_{25}}+\frac{1}{r_{35}}+\frac{1}{r_{45}})+\frac{1}{4}(\frac{1}{r_{13}}+\frac{1}{r_{14}}+\frac{1}{r_{23}}+\frac{1}{r_{24}})\}. \qquad (6)$$

We theoretically set $(A_{\rm 4Q}, \sigma_{\rm 4Q})$ and $(A_{\rm 5Q}, \sigma_{\rm 5Q})$ to be $(A_{\rm 3Q}, \sigma_{\rm 3Q}) \simeq (0.1366, 0.046a^{-2})$ in the 3Q potential [11]. Note that there is no adjustable parameter in the theoretical Ansätze apart from an irrelevant constant.

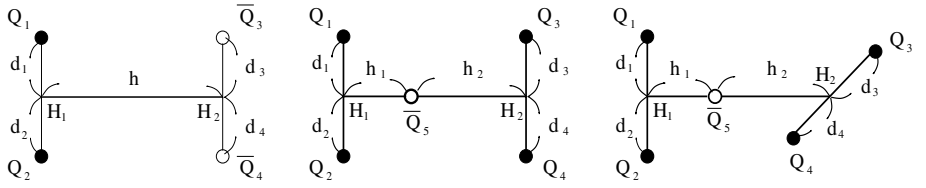

FIGURE 5. (a) A planar tetra-quark (QQ-$\bar{\rm Q}\bar{\rm Q}$) configuration. (b) A planar penta-quark (4Q-$\bar{\rm Q}$) configuration. (c) A twisted penta-quark configuration with $\rm Q_1Q_2 \perp Q_3Q_4$. We here take $d_1 = d_2 = d_3 = d_4 \equiv d$.

Multi-quark Wilson loops and multi-quark potentials

In QCD, static multi-quark potentials can be obtained from the corresponding multi-quark Wilson loops. As shown in Fig.6, we define the 4Q Wilson loop $W_{\rm 4Q}$ and the 5Q

Wilson loop W_{5Q} [15, 16, 17] by

$$W_{4Q} \equiv \frac{1}{3}\mathrm{tr}(\tilde{M}_1\tilde{L}_{12}\tilde{M}_2\tilde{R}_{12}), \quad W_{5Q} \equiv \frac{1}{3!}\varepsilon^{abc}\varepsilon^{a'b'c'}\tilde{M}^{aa'}(\tilde{L}_3\tilde{L}_{12}\tilde{L}_4)^{bb'}(\tilde{R}_3\tilde{R}_{12}\tilde{R}_4)^{cc'}, \quad (7)$$

where $\tilde{L}_i, \tilde{R}_i, \tilde{M}, \tilde{M}_j$ $(i = 1,2,3,4, j = 1,2)$ are given by

$$\tilde{L}_i, \tilde{R}_i, \tilde{M}, \tilde{M}_j \equiv P\exp\{ig\int_{L_i,R_i,M,M_j} dx^\mu A_\mu(x)\} \in \mathrm{SU}(3)_c, \quad (8)$$

i.e., $\tilde{L}_i, \tilde{R}_i, \tilde{M}, \tilde{M}_j$ $(i = 3,4, j = 1,2)$ are line-like variables and $\tilde{L}_i, \tilde{R}_i$ $(i = 1,2)$ are staple-like variables, and $\tilde{L}_{12}, \tilde{R}_{12}$ are defined by

$$\tilde{L}_{12}^{a'a} \equiv \frac{1}{2}\varepsilon^{abc}\varepsilon^{a'b'c'}\tilde{L}_1^{bb'}\tilde{L}_2^{cc'}, \ \tilde{R}_{12}^{a'a} \equiv \frac{1}{2}\varepsilon^{abc}\varepsilon^{a'b'c'}\tilde{R}_1^{bb'}\tilde{R}_2^{cc'}. \quad (9)$$

Note that both the 4Q Wilson loop W_{4Q} and the 5Q Wilson loop W_{5Q} are gauge invariant.

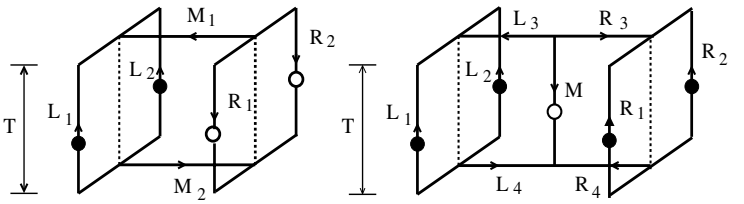

FIGURE 6. (a) The tetra-quark (4Q) Wilson loop W_{4Q}. (b) The penta-quark (5Q) Wilson loop W_{5Q}.

We calculate the multi-quark potentials (V_{4Q}, V_{5Q}) from the multi-quark Wilson loops (W_{4Q}, W_{5Q}) in SU(3) lattice QCD with $\beta = 6.0$ (i.e., $a \simeq 0.1$fm) and $16^3 \times 32$ at the quenched level [15, 16, 17], using the smearing method to reduce excited-state components. In this paper, we investigate planar and twisted configurations for multi-quark systems as shown in Fig.5, and show the results for $d_1 = d_2 = d_3 = d_4 \equiv d$ and $h_1 = h_2 \equiv h/2$.

Figure 7 shows the 4Q potential V_{4Q} [17]. For large h, V_{4Q} coincides with the energy $V_{c4Q}(d,h)$ of the connected 4Q system. For small h, V_{4Q} coincides with the energy $V_{2Q\bar{Q}} = 2V_{Q\bar{Q}}(h)$ of the "two-meson" system composed of two flux-tubes. Thus, we get the relation of $V_{4Q} = \min\{V_{c4Q}(d,h), 2V_{Q\bar{Q}}(h)\}$, and find the "flip-flop" between the connected 4Q system and the "two-meson" system around the level-crossing point where these two systems are degenerate as $V_{c4Q}(d,h) = 2V_{Q\bar{Q}}(h)$.

In Fig.8, we show the 5Q potential V_{5Q}. The lattice data denoted by the symbols are found to be well reproduced by the theoretical curve of OGE plus multi-Y Ansatz [15, 16, 17] with (A_{5Q}, σ_{5Q}) fixed to be (A_{3Q}, σ_{3Q}) in the 3Q potential [11].

As a remarkable fact, we find universality of the string tension and the OGE result among $Q\bar{Q}$, 3Q, 4Q and 5Q systems as [10, 11, 12, 13, 14, 15, 16, 17]

$$\sigma_{Q\bar{Q}} \simeq \sigma_{3Q} \simeq \sigma_{4Q} \simeq \sigma_{5Q}, \quad \frac{1}{2}A_{Q\bar{Q}} \simeq A_{3Q} \simeq A_{4Q} \simeq A_{5Q}. \quad (10)$$

This result supports the flux-tube picture on the confinement mechanism even for multi-quark systems [15, 16, 17].

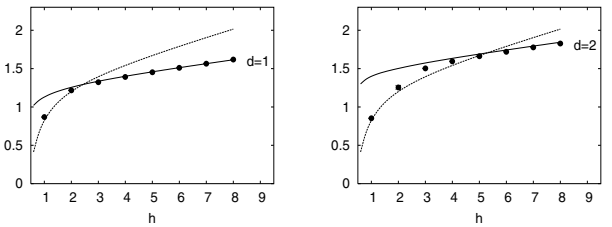

FIGURE 7. The 4Q potential V_{4Q} in the lattice unit for planar 4Q configurations with $d = 1$ (left) and $d = 2$ (right) as shown in Fig.5(a). The symbols denote lattice QCD results. We add the theoretical curves for the connected 4Q system (the solid curve) and for the "two-meson" system (the dashed curve).

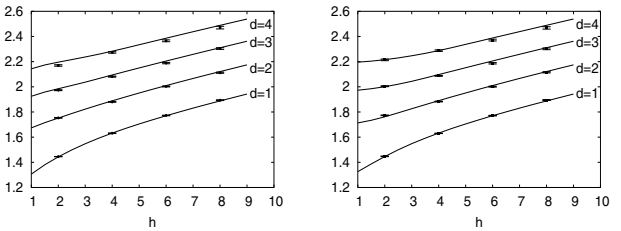

FIGURE 8. The 5Q potential V_{5Q} in the lattice unit for planar configurations (left) and twisted configurations (right) as shown in Figs.5(b) and (c). The symbols denote lattice QCD results. We add the theoretical curve of OGE plus multi-Y Ansatz with (A_{5Q}, σ_{5Q}) fixed to be (A_{3Q}, σ_{3Q}).

5. QCD STRING THEORY FOR PENTA-QUARK DECAY

Our lattice QCD studies on various inter-quark potentials indicate the flux-tube picture for hadrons, which is idealized as the QCD string model. In this section, we consider penta-quark dynamics, especially for its extremely narrow width, in terms of the QCD string theory.

The ordinary string theory mainly describes open and closed strings corresponding to mesons and glueballs, and has only two types of reaction process as shown in Fig.9:

1. String breaking (or fusion) process.
2. String recombination process.

On the other hand, the QCD string theory describes also baryons and antibaryons as Y-shaped flux-tubes, which is different from the ordinary string theory. Note that appearance of Y-type junctions is peculiar to the QCD string theory. Accordingly, the QCD string theory includes third reaction process as shown in Fig.10:

3. Junction (J) and anti-junction ($\bar{\text{J}}$) pair creation (or annihilation) process.

Through this J-$\bar{\text{J}}$ pair creation process, baryon and anti-baryon pair creation can be described.

As a remarkable fact in the QCD string theory, decay process (or creation process) of penta-quark baryons inevitably accompanies J-$\bar{\text{J}}$ creation [26] as shown in Fig.11.

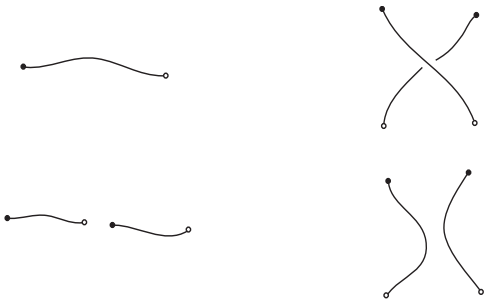

FIGURE 9. Reaction process in the ordinary string theory: string breaking (or fusion) process (left) and string recombination process (right).

FIGURE 10. Junction (J) and anti-junction ($\bar{\text{J}}$) pair creation (or annihilation) process peculiar to the QCD string theory.

Here, the intermediate state is considered as a gluonic-excited state, since it clearly corresponds to a non-quark-origin excitation.

Our lattice QCD study indicates that such a gluonic-excited state is a highly-excited state with an excitation energy above 1GeV. Then, in the QCD string theory, the decay process of penta-quark baryons near the threshold can be regarded as a quantum tunneling, and therefore the penta-quark decay is expected to be strongly suppressed. This leads to a very small decay width of penta-quark baryons.

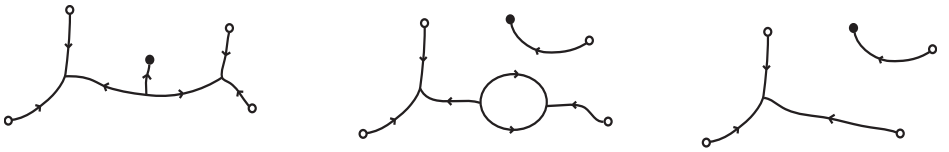

FIGURE 11. A decay process of penta-quark baryons in the QCD string theory. The penta-quark decay process inevitably accompanies J-$\bar{\text{J}}$ creation, which is a kind of gluonic excitation.

Now, we try to estimate the decay width of penta-quark baryons near the threshold in the QCD string theory. In the quantum tunneling as shown in Fig.11, the barrier height corresponds to the gluonic excitation energy ΔE of the intermediate state, and can be estimated as $\Delta E \simeq 1$GeV. The time scale T for this tunneling process is expected to be hadronic scale as $T = 0.5 \sim 1$fm, since T cannot be smaller than the spatial size of the reaction area due to causality. Then, the suppression factor for this penta-quark decay can be roughly estimated as

$$\left|\exp(-\Delta E T)\right|^2 \simeq \left|e^{-1\text{GeV}\times(0.5\sim 1)\text{fm}}\right|^2 \simeq 10^{-2} \sim 10^{-4}. \tag{11}$$

Note that this suppression factor $\left|\exp(-\Delta E T)\right|^2$ appears in the decay process of low-lying penta-quark baryons for both positive-parity and negative-parity states.

For the decay of $\Theta^+(1540)$ into N and K, the Q-value Q is $Q = M(\Theta^+) - M(\mathrm{N}) - M(\mathrm{K}) \simeq (1540 - 940 - 500)\mathrm{MeV} \simeq 100\mathrm{MeV}$. In ordinary sense, the decay width is expected to be controlled by $\Gamma_{\mathrm{hadron}} \simeq Q \simeq 100\mathrm{MeV}$. Considering the extra suppression factor of $|\exp(-\Delta ET)|^2$, we get a rough order estimate for the decay width of $\Theta^+(1540)$ as $\Gamma[\Theta^+(1540)] \simeq \Gamma_{\mathrm{hadron}} \times |\exp(-\Delta ET)|^2 \simeq 1 \sim 10^{-2}\mathrm{MeV}$.

ACKNOWLEDGMENTS

H.S. would like to thank Profs. G.M. Prosperi and N. Brambilla for their kind hospitality at Confinement VI. H.S. is also grateful to Profs. T. Kugo and A. Sugamoto for useful discussions on the QCD string theory. The lattice QCD Monte Carlo simulations have been performed on NEC-SX5 at Osaka University and on HITACHI-SR8000 at KEK.

REFERENCES

1. Y. Nambu, in *Preludes in Theoretical Physics*, (North-Holland, Amsterdam, 1966).
2. M.Y. Han and Y. Nambu, *Phys. Rev.* **139**, B1006 (1965).
3. Y. Nambu, in *Symmetries and Quark Models* (Wayne State University, 1969); *Lecture Notes at the Copenhagen Symposium* (1970).
4. Y. Nambu, *Phys. Rev.* **D10**, 4262 (1974).
5. For instance, articles in *Color Confinement and Hadrons in Quantum Chromodynamics*, edited by H. Suganuma *et al.* (World Scientific, 2004).
6. Y. Nambu and G. Jona-Lasinio, *Phys. Rev.* **122**, 345 (1961); *ibid.* **124**, 246 (1961).
7. M. Creutz, *Phys. Rev. Lett.* **43**, 553 (1979); *ibid.* **43**, 890 (1979); *Phys. Rev.* **D21**, 2308 (1980).
8. H.J. Rothe, *Lattice Gauge Theories*, 2nd edition (World Scientific, 1997) p.1.
9. T.T. Takahashi, H. Matsufuru, Y. Nemoto and H. Suganuma, in *Dynamics of Gauge Fields*, Tokyo, Dec. 1999, edited by A. Chodos *et al.*, (Universal Academy Press, 2000) 179; H. Suganuma, Y. Nemoto, H. Matsufuru and T.T. Takahashi, *Nucl. Phys.* **A680**, 159 (2000).
10. T.T. Takahashi, H. Matsufuru, Y. Nemoto and H. Suganuma, *Phys. Rev. Lett.* **86**, 18 (2001).
11. T.T. Takahashi, H. Suganuma, Y. Nemoto and H. Matsufuru, *Phys. Rev.* **D65**, 114509 (2002).
12. T.T. Takahashi and H. Suganuma, *Phys. Rev. Lett.* **90**, 182001 (2003).
13. T.T. Takahashi and H. Suganuma, *Phys. Rev.* **D70**, 074506 (2004).
14. H. Suganuma, T.T. Takahashi and H. Ichie, in *Color Confinement and Hadrons in Quantum Chromodynamics*, (World Scientific, 2004) p.249; *Nucl. Phys.* **A737** (2004) S27.
15. H. Suganuma, T. T. Takahashi, F. Okiharu and H. Ichie, in *QCD Down Under*, March 2004, Adelaide, *Nucl. Phys.* **B** (Proc. Suppl.) (2004) in press.
16. F. Okiharu, H. Suganuma and T. T. Takahashi, "First study for the pentaquark potential in SU(3) lattice QCD", hep-lat/0407001.
17. F. Okiharu, H. Suganuma, T. T. Takahashi, in *Pentaquark04*, July 2004, SPring-8, Japan (World Sci.).
18. R. Sommer and J. Wosiek, *Phys. Lett.* **149B**, 497 (1984); *Nucl. Phys.* **B267**, 531 (1986).
19. J. Kogut and L. Susskind, *Phys. Rev.* **D11**, 395 (1975); J. Carlson, J. Kogut and V. Pandharipande, *Phys. Rev.* **D27**, 233 (1983); *ibid.* **D28**, 2807 (1983).
20. M. Fable de la Ripelle and Yu. A. Simonov, *Ann. Phys.* **212**, 235 (1991).
21. N. Brambilla, G.M. Prosperi and A. Vairo, *Phys. Lett.* **B362**, 113 (1995).
22. H. Ichie, V. Bornyakov, T. Streuer and G. Schierholz, *Nucl. Phys.* **A721**, 899 (2003); *Nucl. Phys.* **B** (Proc. Suppl.) **119**, 751 (2003).
23. D.S. Kuzmenko and Yu. A. Simonov, *Phys. Atom. Nucl.* **66**, 950 (2003).
24. J.M. Cornwall, *Phys. Rev.* **D69**, 065013 (2004).
25. For a recent review, S. L. Zhu, *Int. J. Mod. Phys.* **A19**, 3439 (2004) and references therein.
26. M. Bando, T. Kugo, A. Sugamoto and S. Terunuma, *Prog. Theor. Phys.* **112**, 325 (2004).